XXI IMEKO World Congress "Measurement in Research and Industry"
August 30 – September 4, 2015, Prague, Czech Republic

NUMERICAL MODELING OF HYSTERESIS APPLIED ON FORCE TRANSDUCER

Thierry Rabault [1], *Philippe Averlant* [1], *Frédéric Boineau* [1]

[1] LNE, 1 rue Gaston Boissier, 75724 Paris Cedex 15, France, email: thierry.rabault@lne.fr

Abstract – When we need to calibrate a force transducer, we usually refer to ISO 376. This standard considers hysteresis as an error included into the uncertainty budget. The objective of this paper is to provide laboratories with tools to estimate the hysteresis. The measurements procedure, the methodology to extract the hysteresis while empowering the zero drift and non-linearity of the calibrated transducer, the modelling and the correction of its effect are proposed.

Keywords: Hysteresis, Reversibility, Transducer, Maxwell-Slip, Calibration.

1. INTRODUCTION

The aim of this article is to give some tools for modelling the hysteresis of standard and industrial force transducers and thus to reduce the measurement uncertainty by correcting its effect, rather than considering it as a non applied correction. When calibrating a force transducer by direct comparison, the application of the hysteresis correction on the standard transducer allows a more accurate assessment of the hysteresis effect on the calibrated one.

In this paper, a method to extract the hysteresis is presented. Algorithms proposed in the literature for different disciplines, are applied for modelling the hysteresis of force transducers. Numerous experimental data provided by several European National Metrology Institutes (NMIs), in the frame of the EMRP project SIB63, allowed us to state the relevance of the studied algorithms.

2. MEASUREMENT PROCEDURE AND REVERSIBILITY EXTRACTION

One measurement cycle by increasing and decreasing force steps, with several previous preload cycles are required to estimate a transducer's hysteresis. Within this cycle, the duration of each applied force should be sufficiently long to eliminate the creep effect. The number of steps should be at least five, distributed as evenly as possible, between the zero and the full scale (*FS*) of the transducer and the same steps are used in the increasing and decreasing phase respectively. (Fig. 1).

For this study, we relied on ISO 376 which recommends to preload the transducer to the maximum capacity three times and to maintain the full load between 60 s and 90 s. The following hysteresis cycle comprises a minimum of eight force steps applied between 30 and 60 seconds.

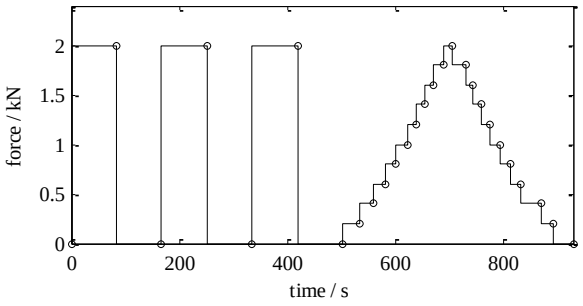

Fig. 1. Procedure for hysteresis evaluation; circles represent the measurements points.

Let's denote $y(t)$ the transducer output signal corresponding to the applied $x(t)$. For $x(t)=0$, the offset in the output signal that may occur is subtracted. The first stage is to calculate the deviation $h_1(t)$ of the signal $y(t)$ from the straight line passing through the origin and the point (x_{max}, y_{max}). We will denote S the apparent sensitivity of the transducer given by the slope of the straight line. It is likely to observe a drift at the end of the cycle which is attributed a zero drift; in this case, $h_1(t)$ is corrected from this drift, considering it is proportional with time, to obtain the hysteresis loop $h_2(t)$.

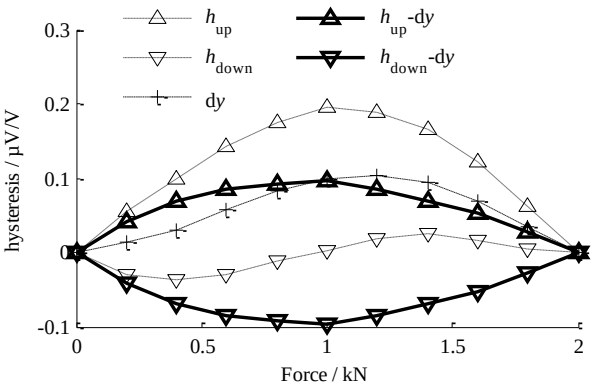

Fig. 2. Graphical representation of the hysteresis deviation dh obtained by the difference of upward h_{up} and downward h_{down} hysteresis, subtracted from the linearity deviation dy.

$h_2(t)$ can be broken down two curves: the hysteresis for an increasing load h_{up} and a decreasing load h_{down}. If we

calculate the average of the ascending curve and the descending curve (h_{up} + h_{down})/2, we get the linearity deviation dy. By subtracting this deviation on h_2(t), we get the perfectly symmetrical hysteresis deviation dh= $|h_{up}$–d$y|$ = $|h_{down}$ –d$y|$ (Fig. 2).

Measurements were made by several European National Metrology Institutes (NMIs), on transducers from six manufacturers (Table 1) and for several measuring ranges (Table 2). The hysteresis deviation dh normalized by the transducer's full scale is plotted versus the normalised applied force on the graph (Fig. 3) for 16 measurements selected amongst 78.

Table 1. Identification of curves, NMIs and manufacturers.

NMI	AEP	BLH	GTM	HBM	MICRO-TEST	Tedea Huntleigh
A		77	74	75	76	
B				3, 4, 5, 6, 7, 8, 9, 10, 11, 12, 13, 14, 15, 16, 17, 18, 19, 20, 21, 22, 23, 24, 25, 26, 27, 28, 29		
C				64, 65, 66, 67, 68, 69, 70		
D				78		
E			71, 73	72		
F			30, 31, 32, 33, 34, 35, 36, 37, 38, 39, 40, 41	42, 43, 44, 45, 46, 47, 48, 49, 50, 51, 52, 53, 54, 55, 56, 57, 58, 59, 61		60
G	62			1, 2		
H			63			

Table 2. Identification of curves, measuring ranges

Range / kN	No. curve
<10	6, 7, 8, 9, 10, 11, 12, 13, 14, 15, 19
10	16, 17, 18, 64, 71
20	20, 21, 26, 27, 28, 30, 31, 32, 33, 65
50	29, 34, 35, 36, 37, 38, 39, 40, 41, 66
100	22, 23, 48, 49, 50, 51, 52, 53, 54, 55, 56, 57, 72
200	24, 25, 58, 59
500	4, 5, 60, 61, 78
1000	3, 42, 43, 44, 45, 46, 47, 67, 68, 69, 74, 75
2000	73, 76, 77
3000	1, 62, 63, 70
5000	2

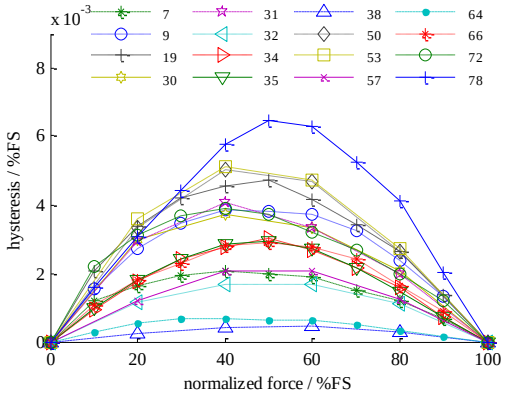

Fig. 3. Comparison of hysteresis deviation for 20 measurements made by several NMI, and for different force ranges between 1 kN up to 1000 kN.

Figure 3 shows an hysteresis deviation as high as $5.10^{-5} \times FS$ at the half scale of the transducer, which represents 100 ppm in relative value of this step

The next paragraph deals with the processing of these measurements results in order to determine the most suitable model to correct hysteresis deviation.

3. NUMERICAL MODELLING OF HYSTERESIS

We have selected algorithms which were developed for modelling the hysteresis deviation, such as the model of Dahl [1], LuGre [2,3], Maxwell-Slip [4,5,6,7], Bouc-Wen [8,9,10], in both positive and negative solicitations case, between $-FS$ and $+FS$. Yet, force calibration facilities allow only tension/compression. Consequently the models must be transposed to positive strains between 0 and FS.

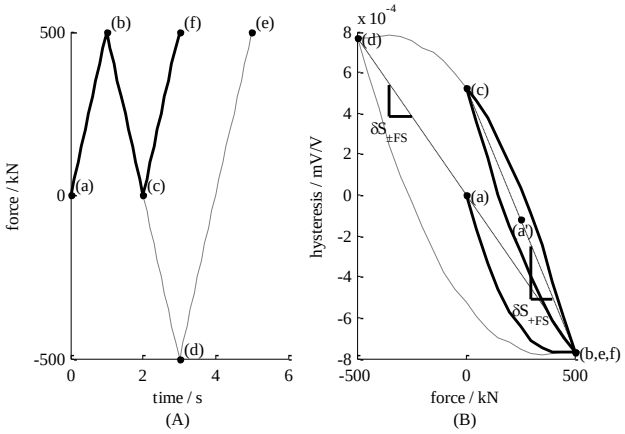

Fig. 4. Test procedure with small hysteresis loops depend on time (A) and displacement (B)

The Figure 4 shows the hysteresis response (Fig. 4A) following a solicitation (Fig 4B). The dash line represents the positive and negative solicitation case and the solid line the truncated positive one. The transition from (a) to (b), corresponding to the rising cycle, is common in both cases, then each solicitation gives an hysteresis loop from (b) to (d) or from (b) to (c), as one can see on the graph B.

After an up-down cycle between 0 and + *FS*, we observe that the signal does not return to its starting point; this offset may explain the zero drift $\delta_z = h_c - h_a$ obtained during a calibration, probably related to the delay associated with the transducer's hysteresis. We also note that the sensitivity $\delta S_{\pm FS}$ for calibration between ± *FS* is different to the one relative to calibration achieved between 0 and *FS*, δS_{+FS}.

The sensitivities are $\delta S_{+FS} = (h_b - h_c)/FS$, and $\delta S_{\pm FS} = (h_b - h_d)/2FS$ respectively (Fig. 4B).

4. MODEL SELECTION

The studied models show an hysteresis envelop with a parabolic shape (Fig. 3). To state the relevance of a model, small variations in the input signal are applied (Fig. 5a). These variations give rise to small hysteresis loops inside the main loop corresponding to the peak-to-peak input signal (Fig. 5b to 5d). The relevance of a model is stated by the ability of the hysteresis signal to recover the main loop after a small one. The Maxwell-Slip model is the most suitable of the studied models, as one can see Fig. 5b to 5d . Moreover, it also best corresponds to experiments (Fig. 6.).

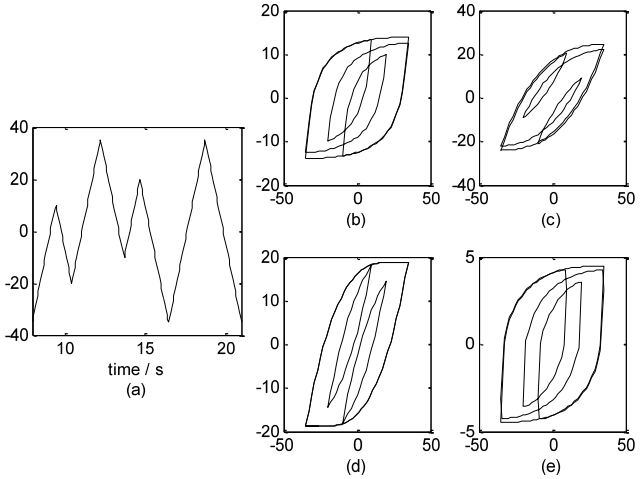

Fig. 5. Comparison of hysteresis models: (b) Dahl model, (c) LuGre model, (d) Maxwell-Slip model and (e) Bouc-Wen model, from the input temporal signal (a).

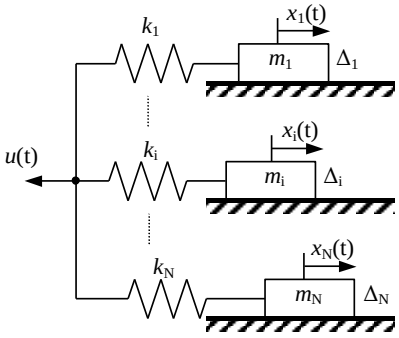

Fig. 6. Maxwell-slip model.

The Maxwell-Slip model considers an assembly of *N* so-called Maxwell cells connected in parallel. Each cell is composed with a mass m_i linked inline with a spring characterized by its stiffness k_i and maximum spring deformation $\Delta_i > 0$ (Fig. 6). The common connection point of the cells is moving a distance *u*(t); $k_i\Delta_i$ is the minimum force to exert on the spring to make the mass mi move. Once the mass is mobile, the force on the spring remains constant to $k_i\Delta_i$ regardless the mass velocity. Consequently, each Maxwell cell is submitted to a friction force $F_i = k_i\Delta_i$. This system can be described with the Duhem model [11]:

$$\dot{x}(t) = \begin{bmatrix} U(-x_i(t) + u(t) - \Delta_i) & U(-x_i(t) + u(t) + \Delta_i) \end{bmatrix} \cdot \begin{bmatrix} \dot{u}_+(t) \\ \dot{u}_-(t) \end{bmatrix} \quad (1)$$

where $\dot{u}_+(t) \cong max\{0, \dot{u}(t)\}$ and $\dot{u}_-(t) \cong min\{0, \dot{u}(t)\}$ are the positive or negative velocity applied to the system.

$$h(t) = \sum_{i=1}^{N} k_i(-x_i(t) + u(t)) \quad i = 1, \ldots, N \quad (2)$$

where *h*(t) is the hysteresis and $U(v) \cong \begin{cases} 1, & v \geq 0, \\ 0, & otherwise. \end{cases}$

5. EXTRACTION OF PARAMETERS

The stiffness k_i and maximum spring deformation Δ_i were determined using measurements on the force transducer HBM type C3H3 at LNE. One cycle by increasing and decreasing force steps was performed without previous preload cycle. Then the hysteresis has been calculated following the method described in the paragraph 2. The slope of the hysteresis' curve is changed in a way the d*h*/d*F* becomes zero for the full scale *FS*, as shown Figure 7.

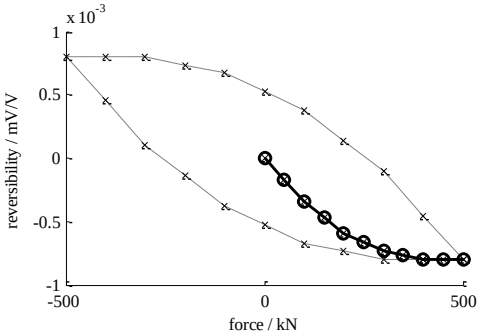

Fig. 7. Response of the force transducer HBM type C3H3, 500 kN.

Let's denote x_i the force levels of the first rising between 0 et 500 kN, indicated by circles in the figure 5 et y_i the corresponding hysteresis values, then: $\Delta_i = x_{1+1}$ and $k_i = (y_{i+1} - y_i)/(x_{i+1} - x_i) - (y_{i+2} - y_{i+1})/(x_{i+2} - x_{i+1})$ with $i = 1, \ldots, N-2$.

6. REVERSIBILITY CORRECTION

To state about the relevance of the parameters (k_i, Δ_i) as determined above, we have performed, on our HBM transducer, a test consisting of three preload cycles followed with one up-and-down cycle between 0 and 500 kN, by step of 50 kN, in which we have included a first loop in the rising phase between 22 and 8 % *FS*, and a second loop in the descending phase, in the same range. The force steps in the loops were reduced to 10 kN to better describe the behaviour at their endpoints (Fig. 8). The hysteresis signal is determined by calculating the root of equation (1) for each measurement point, with the dichotomy technique, until the convergence equals 1×10^{-9}.

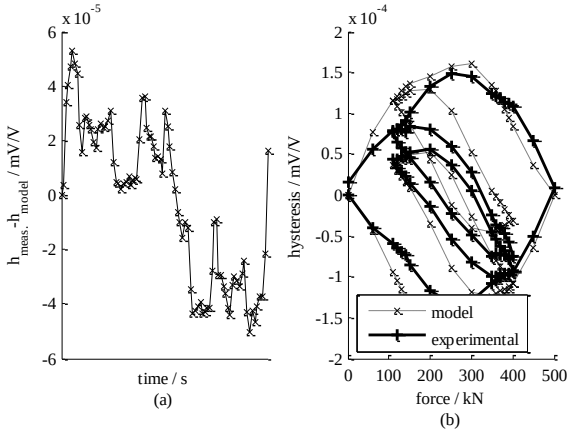

Fig. 8. Comparison between the hysteresis computed with Maxwell-Slip model and the experimental hysteresis using the transducer HBM C3H3.

The Figure 8a plots experimental hysteresis (solid line) and the hysteresis determined from the model (dash line). The difference between these two curves shows a maximum deviation of 5×10^{-5} mV/V for the maximum hysteresis 1.5×10^{-4} mV/V.

7. CONCLUSIONS

This study has highlighted that the Maxwell-Slip model associated to a previous suitable data extraction method was a powerful tool to significantly reduce the hysteresis effect.

We have also observed from this study that the zero drift of a transducer was related to its hysteresis. Further investigations could be conducted from this statement to enhance the developed tool.

ACKNOWLEDGMENTS

The EMRP is jointly funded by the EMRP participating countries within EURAMET and the European Union [12].

REFERENCES

[1] P.R. Dahl, "Measurement of Solid Friction Parameters of Ball Bearings", Technical Report, Aerospace Corp El Segundo, California, 1977.

[2] C.C. De Wit; H. Olsson, K.J. Astrom, P. Lischinsky., "A new model for control of systems with friction," Automatic Control, IEEE Transactions on , Vol.40, No.3, pp.419,425, March 1995

[3] V. Lampaert, J. Swevers, F. Al-Bender , "Comparison of model and non-model based friction compensation techniques in the neighbourhood of pre-sliding friction" American Control Conference, 2004. Proceedings of the 2004 , Vol.2, No., pp.1121,1126 vol.2, June 30 2004-July 2 2004

[4] D.D. Rizos and S.D. Fassois, "Presliding friction identification based upon the Maxwell Slip model structure", Chaos, Vol. 14, No. 2, 2004, pp. 431-445

[5] M. Ruderman and T. Bertram, "Modified Maxwell-slip Model of Presliding Friction", International Federation of Automatic Control (IFAC), Milano (Italy) August 28 - September 2, 2011

[6] F. Al-Bender, V. Lampaert, and J. Swevers, "The Generalized Maxwell-Slip Model: A Novel Model for Friction Simulation and Compensation", IEEE Transactions on Automatic Control, Vol. 50, No. 11, November 2005

[7] V. Lampaert, F. Al-Bender, J. Swevers, "A generalized Maxwell-slip friction model appropriate for control purposes," Physics and Control, International Conference , vol.4, no., pp.1170,1177 vol.4, Aug. 2003, pp. 20-22

[8] R. Bouc, "Forced vibration of mechanical systems with hysteresis". Proceedings of the Fourth Conference on Non-linear Oscilation, Prague,.Czechoslovakia, 1967

[9] Y. K. Wen, "Method for random vibration of hysteretic systems", J. Eng. Mech., Vol. 102, N. 2, March/April 1976, pp. 249-263

[10] S. Dobson, M. Noori, Z. Hou, M. Dimentberg and T. Babert, "Modeling and random vibration analysis of sdof systems with asymmetric hysteresis", lnt. J Non-Linear Mechanics. Vol. 32, No.4, pp. 669-680, 1997

[11] J. Oh, A.K. Padthe, D.S. Bernstein, D.D. Rizos, and S.D. Fassois, "Duhem models for hysteresis in sliding and presliding friction", 44th IEEE Conference on Decision and Control, IEEE Press, New York, pp. 12–15, 2005

[12] European Metrology Research Programme (EMRP), http://www.emrponline.eu